Proceedings of the 48th National Conference on Fluid Mechanics and Fluid Power (FMFP)
December 27-29, 2021, BITS Pilani, Pilani Campus, RJ, India.

FMFP2021-10-003

Design and CFD Analysis of Multi Rotor Wind Turbines

Nirav Subhash Dangi[1], S. R. Nikam[2]

[1]Department of Mechanical Engineering, K.J. Somaiya College of Engineering, Mumbai-400077, India
[2]Department of Mechanical Engineering, K.J. Somaiya College of Engineering, Mumbai-400077, India

ABSTRACT:

Wind power is one of the fastest-growing renewable energy technologies, with global installed wind-generation capacity having increased by a factor of almost 75 in the past two decades. The wind turbine rotors are increasing in diameter to achieve higher power output which poses various challenges in terms of parameters such as structural costs, logistics, maintenance and manufacturing standardization. Multi Rotor Wind Turbines are one potential betterment to Single Rotor Wind turbines. The aim of this study is to compare the performance of Multi Rotor Wind Turbine to a Single Rotor Wind Turbine using Computational Methodology. A total of 8 Horizontal Axis wind turbines which vary in terms of number of rotors, the rotor diameter and the placement of rotors, have been modelled using SolidWorks®. The flow simulations are carried out on ANSYS Fluent ®. It is found that a 4 Rotor configuration with rotors placed in a square formation provides an increase in power output by 35% in comparison to its Single Rotor counterpart. Analysis of wake patterns shows that wake recovery is faster in lesser diameter configurations. The drag force is also found to be low in these configurations, which is beneficial in terms of structural costs and tip losses.

Keywords: CFD, Wind, Turbine, Energy, Sustainable

1. INTRODUCTION:

Wind power usage is on the rise worldwide, in part because costs are falling. Global installed wind-generation capacity onshore and offshore has increased by a factor of almost 75 in the past two decades, jumping from 7.5 gigawatts (GW) in 1997 to some 564 GW by 2018, according to IRENA's latest data. Production of wind electricity is doubled between 2009 and 2013, and in 2016 wind energy accounted for 16% of the electricity generated by renewables [1]. The 2030 forecast by Global Wind Energy Council, states that it will be possible to produce about 2110 GW of electricity from wind energy - contributing to a savings in CO2 emissions of 3.3 billion tonnes per year [2]. The future development of wind power presents a great opportunity to achieve low carbon energy.

There are a lot of emerging technologies which are being assessed to further reduce the cost of generating wind power and make it competitive with fossil fuels [3]. The present study focuses on assessing the potential benefits of Multi-rotor wind turbines. A Multi Rotor wind turbine has several wind turbine rotors mounted on a single support structure. With multi-rotor system it is possible to respond to a turbulent wind field across the device, allowing for more efficient generation and with the potential to alleviate loads [3]. There is also the possibility of yawing without the requirement for a separate mechanism. Turbines can be clustered to reduce some electrical costs, but the independent operation of each turbine maximizes overall load reduction [4, 5]. The production process of smaller rotors could be industrialized and could have lower costs [5].

The power output of a wind turbine varies in square proportionality to the rotor radius and in a cubic proportionality to the incoming wind speed. The multi rotor wind turbines can take advantage of the relation with wind speed because of their comparatively small rotor size. They can be operated in heavy wind speeds as well, where long single rotor turbine would not work because of the high structural loads imposed on it due to its long blade. This helps in achieving a greater average power in comparison to their single rotor counterparts [6]. Since the blade weight increases with diameter, the multi rotor wind turbines can be made with reduced blade mass and cost. Due to the smaller size of rotors, logistics, installation, maintenance costs are also reduced. Moreover, in the case of malfunctioning of one rotor, this does not imply any interruption of energy production from the working rotors of the array.

The modelling of an MRS is challenging and needs more development [7,8]. There has been work [9] to develop three and seven rotor concept systems for small scale applications. The most advanced European project exploiting this technology is a 900 kW four rotor turbine developed by Vestas. As there has been a commercial demonstrator of this technology as mentioned above, there is clearly potential for industrial funding of research to bring this technology to maturity, supported by public funding to tackle some of the more fundamental challenges associated with aeroelastic design and control.
Thus, looking at the potential of Multi- rotor wind turbines, we have conducted this study to play our part in help achieving the mission of the entire globe to reach low or zero-carbon energy.

2. LITERATURE REVIEW AND OBJECTIVE

A wind turbine is a device that exploits the wind's kinetic energy by converting it into useful mechanical energy [10, 11]. It basically consists of rotating aerodynamical surfaces (blades) mounted on a hub/shaft assembly, which transmits the produced mechanical power to the selected energy utilizer (e.g., milling or grinding machine, pump, or generator). A control system is usually provided for adjusting blade angles and rotor position

S. Bhattacharyya and H. Chattopadhyay (eds.), *Fluid Mechanics and Fluid Power (Vol. 1)*,
Lecture Notes in Mechanical Engineering, https://doi.org/10.1007/978-981-19-7055-9_1

to face the wind properly. All units are supported by a stiff tower structure, which elevates the rotor above the earth's boundary layer. There are two common types: horizontal-axis and vertical-axis wind turbines. In the former, which dominate today's markets, the blades spin about an axis perpendicular to the tower at its top, while in the latter they spin about the tower axis itself.

Today, the most common design of wind turbine, and the type which is the focus of this study, is the horizontal axis wind turbine (HAWT). HAWT rotors are usually classified according to the rotor orientation, upwind or downwind of the tower, hub design (rigid or teetering), rotor control (pitch vs. stall), number of blades (usually two or three blades), and how they are aligned with the wind (free yaw or active yaw).

The future development of wind power presents a significant opportunity in terms of providing low carbon energy. It also presents several challenges. It needs to be cost competitive compared with the use of fossil fuels and other competitor renewable energy sources, most notably solar photovoltaics.

The main objectives of this study are:

- To test several configurations of Horizontal Axis Multi Rotor Wind Turbines by use of design and simulation software;
- To establish the configurations by varying the number of rotors and their placements as well;
- To evaluate them on the basis of parameters of Wake Patterns, power output, structural cost estimations, overall power output in a wind farm array;
- To thoroughly compare these configurations with a Horizontal Axis Single Rotor Wind Turbine.

3. METHODS

3.1. Design methods:

The Horizontal-axis wind turbine has been finalised and a total of 8 configurations are designed using parameters set for a Betz optimum blade. For a single rotor configuration, a rotor diameter of 6m is chosen and the corresponding Power in the wind is evaluated with the help of Equation 1 [10], where ρ is density in kgm^{-3}, U is the free stream wind velocity in ms^{-1}, and A is the rotor swept area. The free stream wind velocity is set as 10m/s for all configurations. The choice of diameter is set such that the Fluid domain size is practical with the computational resources available. The rotor diameter for the multi rotor configurations is set such that the Power in the wind remains the same in all configurations. The Rotor power coefficient is then calculated by the results from Flow simulations.

$$\textbf{Rotor power coeffecient} = C_p = \frac{P}{{}^{1}/_{2} * \rho * U^3 * A}$$

An important factor for the design of wind turbines is the tip speed ratio, which is given by Equation 2, where R is the radius of the wind turbine rotor.

$$\textbf{Tip speed ratio} = \lambda = \frac{\omega * R}{U}$$

The chord and twist distributions for the configurations are decided using the parameters set for a Betz optimum blade [10]. Figures 3 and 4 represent the two configurations, Configuration 1 is the base configuration against which the other configurations are compared. The other 3-Dimensional configurations are designed in a similar fashion using SolidWorks®.

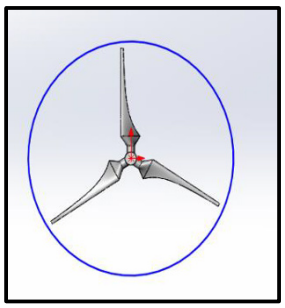

Figure 3:Configuration 1

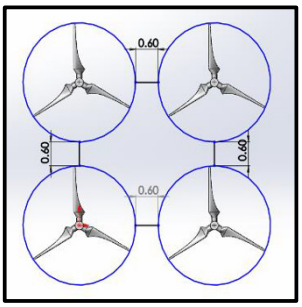

Figure 4: Configuration 4

The airfoils for various sections of the blades are decided from the database of the National Renewable Energy Laboratory (NREL) [12] and an online tool for airfoils [13]. The distance between consecutive rotors for the configurations 2 to 8 is taken as 0.2*D, where D is the diameter of the rotor [14]. 3, 4 and 5 rotor configurations involve change in placement of rotors as well. The change in wake patterns and the power output varies with the placement, thus it was imperative to test them on said basis. Table 1 below shows the details about the configurations.

Table 1: Description of the configurations:

Configuration number and description	Rotor Diameter(m)	Angular velocity (rad/s)
1. Single rotor configuration (Base model)	6	28
2. Two Rotor configuration with rotors placed horizontally	4.3	39.326
3. Three Rotor configuration with rotors placed horizontally	3.46	48.276
4. Three Rotor configuration with rotors placed in a triangular formation [7]	3.46	48.276
5.Four Rotor configuration with rotors placed horizontally	3	56
6. Four Rotor configuration with rotors placed in a square formation	3 [7, 8]	56

7. Five Rotor configuration with rotors placed horizontally	2.6	62.5
8. Five Rotor configuration with rotors placed in a X formation	2.6	62.5

3.2. Analysis methods:

Upon completion of the design phase, the analysis is conducted on the 8 configurations. Computational methodology is chosen, which brings into play Computational Fluid dynamics (CFD) [15]. Firstly, the fluid domain is generated using ANSYS Spaceclaim ®. For the configuration 1, three different domains are made to conduct mesh independence test. These domains include different types of refinements and thus the no. of mesh elements varied in each. For the flow simulation on these domains, ANSYS Fluent ® is used. The results are post processed and the domain size is finalized (Table 2 and 3). The result validation is conducted on ANSYS CFD-Post ® and an open-source wind turbine design software, Q-Blade ® [16]. The final domains contain 2 cylindrical regions, out of which one is the domain in close proximity to the rotor and the other is the rest of the enclosure, and 2 bodies of influence.

Next, a surface mesh was created and different local sizing were tested to find the one which was able to capture all the details of the rotor geometry. After successful surface mesh creation, the volume mesh was generated. For the volume mesh, ANSYS Fluent ® provides a variety of options: Tetrahedral, Polyhedral, Hexcore and Poly- Hexcore. In this study, Poly- Hexcore mesh has been employed due to the benefits it offers [17]. The boundary layer inflation has been done using scoped prisms. A total of 8 layers were generated and the first cell was such that the Y- plus value of ~150 is achieved [18]. This Y- plus was chosen in accordance with the use of Spalart Allmaras turbulence model [19]. The mesh sizing is done such that a fair compromise is obtained between computational feasibility and solution accuracy. A successful mesh is generated on all configurations with all the aerodynamic surfaces being captured fully and necessary refinements in wake region using bodies of influence.

Next, the solver setup is done. Table 4 shows the same. For the turbulence model, the most suitable ones for the simulation of a Wind turbine are the k-ω SST, the k-ε and the Spalart Allmaras models [5, 21]. The k-ω SST model requires a near wall approach which demands a number of cells in the boundary layer to fulfil the condition of Y-plus ≤ 1. Due to limitations in computing power, the use of k-ω SST model is not feasible, thus the final choice is between the k-ε and the Spalart Allmaras model. Simulations were run using both the models and the results monitors are observed. It was found that the simulations faced convergence issues with the k-ε model and thus the results were not getting stable. On the other hand, due to the simplicity of the 1 equation Spalart Allmaras model, the simulations were being conducted smoothly with no issues in convergence. Thus, the Spalart Allmaras model was finalized for the further simulations, with a Y-plus value of ~150. The first cell height required for this value for the different configurations was determined with the help of an open-source online calculator [18]. The Spalart-Allmaras model is a relatively simple one-equation model that solves a modelled transport equation for the kinematic eddy (turbulent) viscosity. This embodies a relatively new class of one-equation models in which it is not necessary to calculate a length scale related to the local shear layer thickness. The Spalart-Allmaras model was designed specifically for aerospace applications involving wall-bounded flows and has been shown to give good results for boundary layers subjected to adverse pressure gradients. It is also gaining popularity in the turbomachinery applications [19].

Governing equations for CFD:

Navier Stokes equations (Excluding Energy):

$$\textbf{Continuity}: \frac{\partial \rho}{\partial t}+\frac{\partial(\rho u)}{\partial x}+\frac{\partial(\rho v)}{\partial y}+\frac{\partial(\rho w)}{\partial z}=0$$

$$\boldsymbol{X-Momentum}: \frac{\partial(\rho u)}{\partial t}+\frac{\partial(\rho u^2)}{\partial x}+\frac{\partial(\rho uv)}{\partial y}+\frac{\partial(\rho uw)}{\partial z} = -\frac{\partial p}{\partial x}+\frac{1}{Re}\left[\frac{\partial \tau_{xx}}{\partial x}+\frac{\partial \tau_{xy}}{\partial y}+\frac{\partial \tau_{xz}}{\partial z}\right]$$

$$\boldsymbol{Y-Momentum}: \frac{\partial(\rho v)}{\partial t}+\frac{\partial(\rho uv)}{\partial x}+\frac{\partial(\rho v^2)}{\partial y}+\frac{\partial(\rho vw)}{\partial z} = -\frac{\partial p}{\partial y}+\frac{1}{Re}\left[\frac{\partial \tau_{xy}}{\partial x}+\frac{\partial \tau_{yy}}{\partial y}+\frac{\partial \tau_{yz}}{\partial z}\right]$$

$$\boldsymbol{Z-Momentum}: \frac{\partial(\rho w)}{\partial t}+\frac{\partial(\rho uw)}{\partial x}+\frac{\partial(\rho vw)}{\partial y}+\frac{\partial(\rho w^2)}{\partial z} = -\frac{\partial p}{\partial z}+\frac{1}{Re}\left[\frac{\partial \tau_{xz}}{\partial x}+\frac{\partial \tau_{yz}}{\partial y}+\frac{\partial \tau_{zz}}{\partial z}\right]$$

where, (x, y, z) are the coordinates, t is time, Re is Reynolds number ρ is density, , τ is stress and (u, v, w) are the velocity components

Transport equtaion of Spalart − Allmaras model **[19]**:

$$\frac{\partial(\rho\tilde{\nu})}{\partial t}+\frac{\partial(\rho\tilde{\nu}u_i)}{\partial x_i} = G_\nu+\frac{1}{\sigma_{\tilde{\nu}}}\left[\frac{\partial}{\partial x_j}\left\{(\mu+\rho\tilde{\nu})\frac{\partial\tilde{\nu}}{\partial x_j}\right\}+C_{b2}\rho\left(\frac{\partial\tilde{\nu}}{\partial x_j}\right)^2\right]-Y_\nu + S_{\tilde{\nu}}, where$$

G_ν is the production of turbulent viscocity, Y_ν is the destruction of turbulent viscocity, $\sigma_{\tilde{\nu}}$ and C_{b2} are the constants, ν is the molecular kinematic viscocity and $S_{\tilde{\nu}}$ is a user defined source term

After the setup, the simulation is run, the convergence plots of the residuals were observed along with result monitors of thrust force and moment. Upon achieving sufficient stability in results, the simulation was stopped (As seen in Figure 5 and 6).

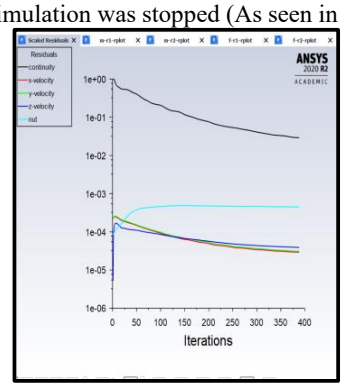

Figure 5: Residuals plot

Table 2: Mesh independence test results

Result Parameter	CFD Domain no.		
	1	2	3
Thrust force (N)	952	945	923
Relative change (%)	3.142	2.384	0
Power coefficient, C_p	0.194	0.182	0.151
Relative change (%)	28.477	20.529	0

Table 3: Dimension of Fluid domain for Configuration 1

Geometry: Configuration 1	X direction (m)		Y direction (m)		Z direction (m)	
	+X	-X	+Y	-Y	+Z	-Z
Enclosure	19	19	19	19	15	48
Body of influence-far	7.5	7.5	7.5	7.5	3	12
Body of influence-near	3	3	3	3	2	2

Table 4: Solver setup

Solver type	Pressure Based and steady state		
Models	Spalart-Allmaras		
Materials	Air	Density(kg/m^3)	Constant at 1.225kg/m^3
		Viscosity(kg/m-s)	Constant at 1.7894e-05 kg/m-s
Cell zone conditions	Enclosure	Fixed frame	
	Rotating domain (cylindrical domain in close proximity to the rotor)	Frame motion in the Z-axis with the specified angular velocity as per the configuration (from Table 1)	
	Operating pressure	101325 Pa	
Boundary Conditions	Upstream surface of domain	Velocity inlet	
		Velocity	10 m/s
		Turbulent viscosity ratio	10
	Downstream surface of domain	Outflow	
		Flow rate weighting	1
	Side walls	Symmetry	
	Surfaces of the rotor	No slip walls	
Solution Methods	Pressure-Velocity coupling	Coupled scheme	
	Pseudo Transient	ON	
	Warped Face gradient correction	ON	
	High order term relaxation	ON	
	Spatial Discretization	Gradient	Least Squares cell based
		Pressure	Second Order
		Momentum	Second Order Upwind
		Modified Turbulent viscosity	Second Order Upwind
Solution Controls	Pseudo transient explicit relaxation factors	Pressure	0.8
		Momentum	0.5
		Density	1
		Body forces	1
		Modified Turbulent viscosity	0.75
		Turbulent viscosity	1
Initialization	Standard		
Calculation	Time step method	Automatic	
	Length scale method	Conservative	
	Time scale factor	1	

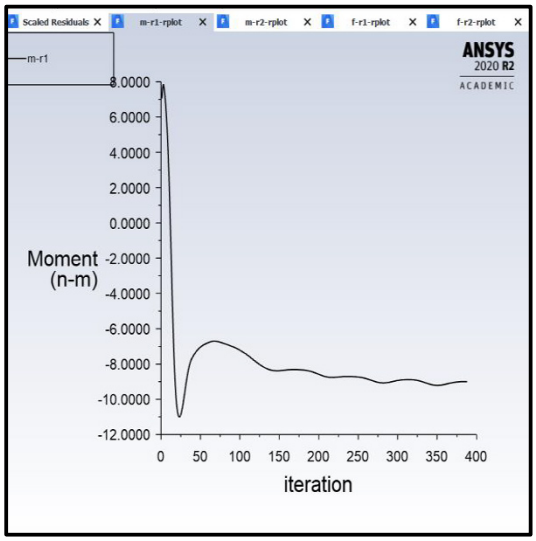

Figure 6: Moment monitor plot for configuration 2

5. RESULTS AND DISCUSSION

The flow simulation for all the configurations is run with the setup as discussed above. Values of Torque are obtained using the simulation, which is used to calculate the available power output as shown in Table 5 below. The configuration 6 is seen to outperform all the other configurations with an increase in the power coefficient by ~35% over the single rotor configuration 1. This is a substantial increase in power output which when employed in a Wind farm array will be able to produce a very high overall power output in comparison to its single rotor counterpart. Configuration 4 which is a 4-rotor configuration wherein the rotors are placed in a square formation has shown a great benefit in terms of power output, and since it has a rotor diameter which is 50% less than its single rotor counterpart suggests that the overall loads on this rotor as much less than the configuration 1. With this added benefit, the structural costs could be minimised to a great extent along with a significant advantage in terms of transportation and maintenance. Owing to its low rotor diameter it has been observed that the wake recovery happens in a very short distance thus saving space in a Wind farm array (Evident from Table 5 and calculation explained in Figure 7).

Table 5: Results from flow simulation:

Configuration No.	Torque from CFD Results (τ)	Power of 1 rotor ($P = \tau * \omega$)	Power coefficient (C_p) obtained	Relative change in Power output with respect to Configuration 1	Thrust	Wake recovery distance
	(N-m)	(W)			(N)	(m)
1	65	1820	0.151	0	923	13.5
2	20.25	796.348	0.131	-13.687 %	487	11
3	15.14	730.897	0.181	+ 19.381 %	315	8.2
4	13.69	660.897	0.163	+ 7.947%	319	8.1
5	10.55	590.8	0.196	+ 29.847 %	220	8
6	10.98	614.88	0.204	+ 35.14%	220	7.8
7	5.58	348.75	0.144	- 4.524%	206	7.7
8	6.92	432.5	0.179	+ 18.404 %	206	7.4

A similar nature of results has been noted in [20] as well. With this attribute, there will be a benefit in terms of placement of wind turbines is arrays. The next wind turbine in a multi rotor configuration can be placed closer to that in comparison to a single rotor configuration. This would enable more wind turbines in the same space of a wind farm and thus increasing available power output. The larger distance in terms of rotor diameter is due to the higher rotational velocities of the blades in the multi rotor configurations. With the reduced thrust value reduces attributed to the fact that the rotational velocity is higher in the configurations with smaller rotor diameter, the cost of production will likely be reduced due to the lower loads.

6. CONCLUSIONS

The various configurations have been modelled using CAD Software. The CFD Analysis has been successfully completed and the power output of each configuration has been tabulated. The results have been validated to ensure the accuracy of the results. It has been inferred that on basis of power output, the configuration 6 outperforms the other configurations. It provides a ~35% increase in power output because of the increase in power coefficient. Upon analysing the wake patterns, it has been found that as the rotor diameter decreases the wake normalisation takes place earlier thus suggesting in possibility of placing the next turbine in the array closer to it than in comparison to a large diameter turbine. Due to lower thrust forces on lesser diameter configurations, we see a benefit in terms of structural costs as the blade will not be required to carry excessive loads that are accompanied with higher thrust values. Due to their lower size, a benefit in terms of transportation and maintenance has been noted as well. This shows how beneficial the Multi Rotor wind turbines can be in comparison to their Single Rotor counterpart. The various

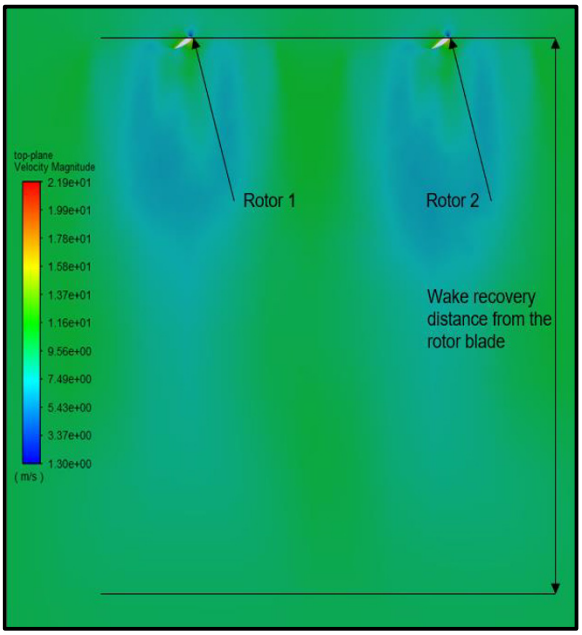

Figure 7: Velocity contour for Configuration 2

benefits have been discussed in Results Section as well. Thus, upon realising the benefits of the Multi rotor wind turbines, we would like to promulgate further work on the study by incorporating the limitations discussed previously.

REFERENCES

[1] The International Renewable Energy Agency (IRENA): Renewable Capacity Statistics 2019, March 2019, ISBN : 978-92-9260-123-2

[2] Global Wind Energy Outlook 2016: Wind Power to dominate power sector growth. Global Wind Energy Council. [Online] 2016. https://gwec.net/publications/global-wind-energy-outlook/global-wind-energy-outlook-2016/

[3] Simon Watson, Alberto Moro and Vera Reis, Future emerging technologies in the wind power sector: European perspective, Renewable and Sustainable Energy Reviews, Elsevier, 2019, https://doi.org/10.1016/j.rser.2019.109270

[4] Jamieson P, Branney M, Chaviaropoulos P, Sieros G, Voutsinas S, Chasapogiannis P. The structural design and preliminary aerodynamic evaluation of a multi-rotor system as a solution for offshore systems of 20 MW or more unit capacity. J Phys Conf Ser 2014; 5241:012084

[5] Jamieson P, Branney M, Hart K, Chaviaropoulos PK, Sieros G, Voutsinas S, et al. Innovative turbine concepts - deliverable 1.33 of the EU INNWIND project. 2015

[6] Peter Jamieson and Michael Branney, Multi-Rotors; A Solution to 20MW and Beyond, DeepWind, 19-20 January 2012, Trondheim, Norway

[7] Chasapogiannis P, Prospathopoulos JM, Voutsinas SG, Chaviaropoulos TK. Analysis of the aerodynamic performance of the multi-rotor concept. J Phys Conf Ser 2014; 524:012084. https://doi.org/10.1088/1742-6596/524/1/012084

[8] Verma, Preeti, "Multi Rotor Wind Turbine Design And Cost Scaling" (2013).Masters Theses 1911 - February 2014. 1158

[9] Goltenbott U. Aerodynamics of multi-rotor wind turbine systems using diffuser augmentation PhD Thesis Kyushu University; 2017. https://doi.org/10.15017/ 1807035.

[10] J. F. Manwell, J. G. McGowan and A. L. Rogers, Wind Energy Explained: Theory, Design and Application, 2009 John Wiley & Sons Ltd., ISBN 978-0-470-01500-1

[11] Tony Burton, David Sharpe, Nick Jenkins and Ervin Bossanyi, Wind Energy Handbook, 2001, John Wiley and Sons, Ltd., ISBN 0-471-48997-2

[12] NREL, National Renewable Energy Laboratory's National Wind Technology Centre: Wind Turbine Airfoil list; https://wind.nrel.gov/airfoils/AirfoilList.html

[13] Airfoil Tools: Tools to search, compare and plot airfoils, http://airfoiltools.com/

[14] Majid Bastankhah and Mahdi Akbar, Multirotor wind turbine wakes, Phys. Fluids 31, 085106 (2019); https://doi.org/10.1063/1.5097285

[15] Simscale Documentation, Computational Fluid Dynamics, February, 2021: https://www.simscale.com/docs/simwiki/cfd-computational-fluid-dynamics/what-is-cfd-computational-fluid-dynamics/

[16] QBlade Wind turbine design and simulation: http://www.q-blade.org/

[17] Linkedin, Better meshing using ANSYS Fluent ® Meshing? post by Leap Australia, accessed April 2020, https://www.linkedin.com/pulse/better-meshing-using-ansys-fluent-hashan-mendis

[18] Leap Australia, "Tips & Tricks: Estimating The First Cell Height For Correct Y+", accessed June 2020, https://www.computationalfluiddynamics.com.au/tips-tricks-cfd-estimate-first-cellheight/

[19] ANSYS Fluent ® Guide, " Overview of Spalart Allmaras Model", accessed July 2020, https://www.afs.enea.it/project/neptunius/docs/fluent/html/th/node49.htm

[20] Sandip A. Kale and S. N. Sapali, A Review of Multi-Rotor Wind Turbine Systems, Journal of Sustainable Manufacturing and Renewable Energy, Volume 2 Number 1/2, Nova Science Publishers, Inc., ISSN: 2153-6821

[21] Alireza Shourangiz-Haghighi, Mohammad Amin Haghnegahdar, Lin Wang, Marco Mussetta, Athanasios Kolios and Martin Lander, State of the Art in the Optimisation of Wind Turbine Performance Using CFD, Archives of Computational Methods in Engineering, Springer, CIMNE, Barcelona, Spain 2019, https://doi.org/10.1007/s11831-019-09316-0